Roughness influence on the optical properties and scratch behavior of acrylic coating deposited on sandblasted glass

Hind Laouamri, Sylvain Giljean, Gilles Arnold, Mostafa Kolli, Nourredine Bouaouadja, Marie-Helene Tuilier

▶ **To cite this version:**

Hind Laouamri, Sylvain Giljean, Gilles Arnold, Mostafa Kolli, Nourredine Bouaouadja, et al.. Roughness influence on the optical properties and scratch behavior of acrylic coating deposited on sandblasted glass. Progress in Organic Coatings, 2016, 101, pp.400-406. 10.1016/j.porgcoat.2016.09.014 . hal-03110971

HAL Id: hal-03110971
https://hal.science/hal-03110971v1

Submitted on 4 Apr 2022

HAL is a multi-disciplinary open access archive for the deposit and dissemination of scientific research documents, whether they are published or not. The documents may come from teaching and research institutions in France or abroad, or from public or private research centers.

L'archive ouverte pluridisciplinaire **HAL**, est destinée au dépôt et à la diffusion de documents scientifiques de niveau recherche, publiés ou non, émanant des établissements d'enseignement et de recherche français ou étrangers, des laboratoires publics ou privés.

Roughness influence on the optical properties and scratch behavior of acrylic coating deposited on sandblasted glass

Hind LAOUAMRI[1], Sylvain GILJEAN[2], Gilles ARNOLD[2], Mostafa KOLLI[3], Nourredine BOUAOUADJA[1], Marie-Hélène TUILIER[2]

[1]Non Metallic Materials Laboratory (LMNM) IOMP, Ferhat Abbas University Setif 1, 19000 Algeria.

[2]Université de Haute-Alsace, Laboratoire de Physique et Mécanique Textiles (LPMT - EA 4365), 68093 Mulhouse, France.

[3]Emerging Materials Research Unit (URMES), University Ferhat Abbas Sétif 1, 19000 Algeria.

Corresponding Author: sylvain.giljean@uha.fr

Abstract:

In this work, acrylic coatings were deposited on sandblasted soda-lime glass in order to correct the loss of optical properties. Erosion tests were carried out under normal incidence with a constant sand flow 25 m/s. By varying the projected sand mass, different surface states were obtained. The influence of the roughness on the optical properties and the mechanical behavior of the coating was observed. At the erosion beginning, eroded samples show isolated defects randomly distributed on the surfaces. As the projected sand mass increases, the number and the size of defects increase. Consequently, the optical transmission drops

dramatically from 91.4% (initial value) to 20% after sandblasting with a mass of 200 g, while the arithmetic roughness increases from 0.04 to 2 µm. To correct the damage caused by sandblasting, a 10 µm thick acrylic coating was deposited by spraying. The resultant polymeric coating reduces the surface roughness and improves significantly the optical transmission (90%) which is close to the initial value. Scratch tests were carried out using an increasing normal load to study the adhesion behavior of acrylic coatings deposited on the sandblasted glasses. The results show that the roughness has an influence on the value of the critical load of delamination at the interface coating/substrate. Therefore, the coatings resistance is related to the surface roughness state. The effect of HF-etching of sandblasted glasses on the interfacial adhesion of acrylic-coated glasses was also investigated.

Key words: glass, erosion, adhesion, scratch test, hydrofluoric acid etching

Highlights

- Acrylic coating is used to heal common soda-lime glass after sandblasting
- Acrylic coating restores the optical transmission of damaged glass
- HF-etching pre-treatment increases adhesion of coating
- The best adhesion properties are obtained for an optimal roughness level

Introduction

In Saharan regions, like in many other arid regions, erosion of brittle materials such as ceramics and glasses caused by sandstorms is an important problem to be taken care in term of economic aspect. Generally, glass sandblasting erosion is characterized by the formation of surface microcracks, chipping and sometimes craters. These defects affect the optical quality surface state of glasses and lead to a significant drop in the optical transmission, mainly by diffusion of the incident light [1]. It has been demonstrated that in the case of windscreens, the wear due to small particles erosion can affect driving safety [2]. In the field of solar cells, the durability is also a great preoccupation [3-5]. For this reason, considerable efforts have been made in recent years to deal with this kind of deterioration [1,6-9].

It is well known [10-13] that erosion of brittle materials is influenced by several factors such as: properties of the erodent particles (size, shape, density, hardness and toughness), properties of target material (hardness, toughness) and the experimental conditions (impact speed, impingement angle, projected masses, temperature). In ductile materials, maximum erosion occurs at low impact angle whereas maximum erosion occurs at an angle close to 90° for brittle materials. Numerical models have been proposed to predict the evolution of surface roughness as a function of erosion process parameters [14,15]. Among all these parameters, the velocity, the projected mass and the shape of the incident particles play the main role in the erosion process, since they govern their kinetic energy. The correlation between the optical transmission, the roughness, the light scattering with the surface damage were the object of several works [16-18]. For normal incidence [16], the optical transmission falls from 91.6 to 13% while arithmetic roughness (Ra) increases from 0.035 up to 2.270 μm and a visibility limit was defined at about Ra=1.5 μm.

At the present time, no method exists for completely overcoming the sandblasting damage. However coatings can, partially or completely fill the flaws in glass surfaces and thereby increase the optical and mechanical properties of glass articles [1,6,9].

Polymeric coatings (acrylic, epoxy…) are widely used in buildings, vehicles, bottles and electronic equipments for both functional and aesthetic purposes [19-22]. In the case of solar cells, coating can be used to optimize optical properties such as transmittance and reflectance as well as enhance self-cleaning capacity [23]. Moreover, coating solutions are economically attractive compared with glass tempering or ion exchange technologies [22].

In film-coating processes, adhesion between polymeric film and substrate is a major consideration. Therefore, in the case of both organic and inorganic coatings, a special attention has to be taken to the surface preparation of the glass surface before coating to optimize its adhesion capacity [24,25]. One route consists in modify the surface topology in order to increase the potential contact surface. In the case of pretreated glass by abrasion, it is well known that the adhesion is lower for smooth or coarse surfaces while for intermediate roughness, the bond resistance reaches a max located between 3 and 4 MPa for a surface roughness of 5 µm [26]. It was shown that an increase in surface area results in increasing intermolecular bonds and keying for mechanical adhesion. Another route consists in change the nature of the chemical groups present at the surface. One of the standardized surface treatments, which change both surface topography and chemical bonds, is chemical etching of the glass substrates using aggressive solutions containing hydrofluoric (HF) acid or its derivatives [27-29].

The scratch test is widely used to characterize the film – substrate system. Simple tests can be performed in a first approach using a pencil hardness tester [3]. The use of an instrumented scratch tester enables more accurate results. The test consists in drawing a diamond tip along the coated surface under an increasing load until damage of the coating occurs [25]. The

observation of the scratch gives information on the deformation and damage mechanisms [30-32] and quantitative characteristics such as crack resistance and adhesive strength can be obtained using models proposed in the literature [33-35].

In this study, the effect of sandblasting on roughness and optical properties of common soda lime glass is presented. Healing of sandblasted glasses is performed by sprayed acrylic coating. The influence of surface roughness on adhesion of the coating is investigated and the effect of a HF acid pre-treatment is also reported.

Experimental procedure

Sandblasting

A common soda-lime glass, manufactured by Africaver (Algeria) was used for experimental test. The mean chemical composition of this glass is presented in Table 1. Samples with dimensions 50x50x3 mm^3 were cut from the same sheet. These samples were sandblasted on one side using a sand blower device. A horizontal jet impingement system was used as recommended by the standards for airborne particles erosion testing (DIN 50 33218 and ASTM G7619). Some details of this device have been given in previous publications [16,17,36].

The eroding material used in this study was sand coming from the desert of Algeria (region of Ouargla) and has already been characterized in previous work [10]. The particle shape varied from spherical in majority to angular. Colored aspect of the sand grains suggested that they had a diversified mineralogical composition. The major minerals composing this sand were brown tourmaline, limonite, colored and uncolored quartz. The sand particle sizes were ranging mainly between 350 and 480 µm. All the erosion tests were carried out under ambient conditions (24.8°C, 42% RH).

The sandblasting tests consisted in exposing the samples to a sand flux under controlled test conditions. In our case, the samples were placed in normal position (90°) relative to the sand flux. The flux rate was kept constant to 1.25 g/s. The velocity value was fixed at 25 m/s according to velocities measured during sandstorms. The only variable parameter was the projected sand mass Mp which varied as: 50, 100, 150 and 200 g (Table 2). In order to characterize the sandblasting levels independently of the size of the sandblasted area, local values have to be considered. Some authors consider the impact density [14] or the projected mass density [37]. A more pertinent parameter to consider is the kinematic energy density [13,14]. Considering a sandblasted area of diameter 40 mm in our experiments, the mean projected mass density and the mean kinematic energy density were assessed.

Chemical treatment (hydrofluoric acid etching)

Half of sandblasted samples were immersed in a solution containing hydrofluoric acid (HF 5%) during 2 minutes. The chemical reaction was performed at ambient temperature and atmospheric pressure using stirring. After that, the samples were rinced with water to remove all residuals from the chemical process.

Coating

The acrylic formulation was obtained through diluting 100 ml of 2K acrylic clear (MaxMeyer Clear 0500: 1.360.0500) by 50 ml of standard thinner for 2K products and MaxiCar HS (MaxMeyer Thinner 4310: 1.911.4310) and 30 ml of MS super rapid hardener (MaxMeyer MS Hardener 9000: 1.954.9000). The mixture was stirred for 2 minutes and sprayed on the glass. Details of coating procedure were given in a previous publication [36]. After drying in an oven at 50 °C for 30 minutes, the resulting coatings were heated at 150 °C for one hour. The final mean thickness of the coating, estimated by tactile profilometry, is about 10 µm.

Characterization

The eroded surfaces were observed with a Scanning Electron Microscope Hitachi S-2360N and with optical microscopy.

Roughness measurements were carried out on a Taylor Hobson tactile profilometer (Model: Form Talysurf Series 120i 2) with a resolution of 16 nm in Z. A stylus having a 2µm tip radius was used. For each sample, at least 5 profiles built with 20000 points were randomly recorded at a speed of 0.5 mm/s on a total length of 15 mm. Arithmetic average roughness Ra and total roughness Rt were calculated with the embedded software.

The samples were analyzed by UV–VIS spectroscopy in the range 200–1100 nm to obtain the transmittance using a Perkin Elmer Spectrometer (type Lambda 950 UV/Vis). The optical transmission was determined at $\lambda = 550$ nm.

The adhesion properties of the acrylic coatings were evaluated using a CSM Micro Instrument Scratch Tester. The indenter was a diamond Rockwell C tip with a radius of 200 µm. The experimental conditions were chosen in order to operate in the optimum accuracy range of the experimental apparatus in terms of load and sensor sensitivity. The scratch length was set to 10 mm; the applied normal load was progressively increased from 0.03 to 7 N at a rate of 2.5 mm/min. This low scratch speed was used to optimize the sensitivity to elastic, plastic and fracture contributions since polymer materials are sensitive to time dependent effects. After the test, critical loads (LC) where a particular failure mode occurred were determined by observations of the scratch track using a built-in optical microscope. At least five measurements were performed at room temperature on each sample. Usually the error on the LC determination is due to two main contributions: a major contribution due to statistical error induced by random distribution of the roughness and another contribution due to the position accuracy of the sample under the microscope that induces an error of some mN.

Results and discussion

Glass morphological changes

Figure 1 presents two micrographs that show the general aspect of damaged glasses with 50 and 200 g of projected sand mass. Microscopic observations indicate that in the first stage of the process, the sandblasted defects are isolated and randomly distributed (figure 1a). As the projected sand mass increases, the number and the size of the defects increase and interactions occur between neighboring defects which lead to the formation of coalescent damaged areas as shown in figure 1b. The phenomenon develops and tends to extend to the entire exposed surface. Mahdaoui et al. showed in their work that soda lime glass erosion produced numerous small chipped zones [38].

The sandblasting morphology flaws evolution was followed by microscopic observations on SEM. Figure 2a presents a general view of a sandblasted and etched glass. The HF-etching leads to dig the asperities and enlarge the radial cracks. This is clearly seen on the observed default which is shown with different magnifications in figures 2b and 2c. These results are in accordance with the findings observed by other authors [7,29].

Roughness

Figure 3 shows the variation of the roughness parameters Ra and Rt in relation to the projected sand mass. The as-received glass has an average roughness Ra and total roughness Rt of 0.04 and 0.23 µm respectively. After sandblasting, the roughness values increase with the projected sand mass and reach Ra = 1.99 ± 0.10 µm and Rt = 17.3 ± 2.0 µm for 200 g of sand. This behavior is quite normal since the presence of surface defects promotes the roughness. Verspui et al. [15] have reported that in the case of borosilicate glass eroded by alumina particles, when a lateral crack breaks out, it induces a clear roughness increasing.

As mentioned earlier, after sandblasting the resulting surface morphology is micro-coarsened. The established morphology is the result of superimposed peaks and valleys, which are generated from the sand impact on the brittle glass surface. Thus the final morphology displays distributed asperities which lead to increase the roughness.

After HF-etching, the as received glass roughness Ra should increase in the order of a tens of nanometers due to chemical reaction with oxides [27]. Such a small increase was not detected because of the resolution of the device. Concerning sandblasted specimens, a surface state degradation in a form of glass scales removal and surface cracks opening is observed (figure 2). This leads to more surface irregularities and therefore to an increase of Ra in the order of the micrometer (figure 3a). The roughness values increases to $Ra = 2.3 \pm 0.3$ µm and $Rt = 20.4 \pm 2.0$ µm for the most degraded case. Etching by hydrofluoric acid produced a rougher surface because of the opening of cracks generated by sandblasting [8,29].

After deposition of acrylic coating, the morphology of both sandblasted and etched samples is significantly modified; the surface roughness of all samples decreases. The acrylic solution infiltrates the surface irregularities, filling the gaps among them. Thus the morphology of damaged glasses becomes smoother. Accordingly, the acrylic coating deposited on sandblasted glass with Mp = 200 g is characterized by Ra and Rt of 0.7 ± 0.2 and 5.8 ± 1.0 µm respectively. For the sandblasted and etched glass after coating, Ra and Rt are 0.90 ± 0.06 and 6.1 ± 1.0 µm respectively. These roughness parameters confirm the smoothing of the eroded glasses after the deposition process.

Optical transmission

Figure 4 shows the variation of the optical transmission versus the projected sand mass, for the different glass states sandblasted and HF-etched. The optical transmission T of the as-received glass was established for $\lambda = 550$ nm at about 91.4 %. After sandblasting, T shows a steady decline from the initial state (undamaged state) up to 200 g where it reaches 20 %. The

microscopic damages generated by sand particle impacts diffuse the incident light and induce a decrease of the optical transmission [39]. For the acid attacked glasses, the transmission drops sharply to 15 % for Mp = 200 g, this corresponds to the most important roughness; which confirms that the optical properties of glass are strongly affected by its surface quality.

Deposition of acrylic coating leads to a remarkable recovery of the optical transmission which reaches about 90 %. This improvement is explained by the filling of the defects sites with the acrylic solution. Its good transparency recovers almost entirely the optical transmission deterioration caused by sandblasting and HF-etching. It may indicate that the sprayed solution fills correctly the cracks opened by sandblasting as previously mentioned independently from the etching pre-treatment.

Adhesion of the acrylic coatings

An example of scratch behavior of the acrylic coatings is shown in figure 5a. Scratch induced successively damages such as non-damage, mar, first crack (figure 5b), coating delamination at the pile up (figure 5c) and scrape off of the coating under the tip or total delamination (figure 5d). Bull et al. [33] has classified those failure modes in terms of substrate and coating hardness and has shown that when a soft coating is deposited on a harder substrate such as acrylic on glass in our case, the coating tends to deform by plastic deformation. It can be expected that the deformation of the glass substrate is negligible as observed in the case of polyurethane coating where no deformation of the glass substrate was observed [30].

At the beginning of scratch on figure 5a, so under low load and stress level, a small amount of permanent deformation is observed. This deformation results from competition of fully recoverable elastic deformation, time–dependent viscoelastic deformation, and a small amount of non-recoverable plastic deformation resulting from compressive indentation which can be called mar [32].

At the end of mar region, the first crack appears in the scratch track. While increasing the scratch normal load, cohesive cracks begin to form and become more regular and dense. The orientation of the scratch and the observation of the end of the track indicate that the fracture occurs at the back of the contact due to tensile stresses [40]. The first critical load LC_1 is defined in this paper as the load at the apparition of the first crack in the layer (figure 5b). The values of the critical loads LC_1 is plotted as a function of roughness on figure 6a for both sandblasted coated samples (SC) and sandblasted etched coated samples (SEC). LC_1 values decrease as the roughness increases. The first crack appears at a critical stress value that depend, for a given normal load value, on the thickness of the layer under the tip. The thickness under the tip can be related to the distribution of peaks and valleys of the roughness. Statistically, the threshold of stress that induces the first crack is reached for lower load values on rough samples.

In the present study, considering that the deformation of the substrate is negligible [30], simple geometrical considerations enable to assess the penetration h of the indenter into the coating as a function of the value of the width $2a$ of the track and of the indenter radius R. At LC_1, the value of a = 40 µm corresponds to a penetration h of approximately 4 µm.

Coating delamination at the pile up (figure 5c) is observed in the load range 2.5 to 3.5 N only on non-etched samples. The HF-etching enables the increase of the scratch resistance of the acrylic coatings. This observation correlates the good results of optical transmission and could indicate that etching, by digging slightly the cracks, enhances the penetration of the solution and therefore the adhesion of the coating.

The last failure mode observed for higher scratch normal load is the removing of the acrylic layer under the tip or even the total delamination of the coating for GC, GEC and 050SC samples (scratches not shown). The second critical load LC_2, defined in this paper, corresponds to the load at the apparition of the removing or delamination of the layer (figure

5d). The values of LC_2 where plotted as a function of roughness on figure 6b for both sandblasted coated samples (SC) and sandblasted etched coated samples (SEC). It can be noticed that largest amplitude for LC_2 values are observed for rougher samples. The scrape off resistance of the coating is higher on rough samples than on as-received glass (GC). The scratch performance of coatings on rough glasses was ascribed to the good mechanical interlocking at the interface promoted by the micro-corrugation [24]. The increase of interfacial adhesion of coatings with substrate roughness was also observed in the case of acrylic coating on polymeric substrates [41]. Accordingly the coating becomes more able to withstand external loading conditions because the presence of internal stresses is mitigated by the corrugated morphological features of the substrate surface itself [42]. The critical load that induce scrape off of the acrylic layer increases with substrate roughness until an optimum of Ra where LC_2 decreases with Ra (figure 6b). This behavior can be explained by the stochastic roughness profile of sandblasted glasses for the most degraded state [24]. Several authors have investigated the effect of surface roughness on adhesion, and a number of concepts have been proposed [26,43]. In the present case, at low roughness, poor adhesion is observed and delamination occurs, while sandblasting has a benefic effect on adhesion up to 150 g and etching has a valuable contribution in the first stage of sandblasting (50 g). Above 150 g (12 g/cm^2), the micro-corrugation tends to saturate as the size of some large asperities lead to facilitate the damage of the coating. To ensure the best scratch resistance, healing of glasses by filing an acrylic coating must be carried out before the surface state is too degraded.

Conclusion

In this paper, acrylic coatings were deposited on sandblasted glasses with different surface roughnesses in order to correct the damage and the loss of optical properties. It was shown that sandblasting of glass leads to an increase in surface roughness and a drop in optical

transmission. Deposition of acrylic coating was beneficial to both the visual appearance of the substrates and the optical transmittance. Scratch test technique was performed and demonstrated that the roughness of the substrates has an influence on the crack resistance of the coating and on delamination or scrape off resistance. HF-etching pre-treatment, used to improve acrylic coating adhesion, showed no significant effect on optical transmission while exhibited an effect on interfacial adhesion especially at the pile-up. Finally the results showed that healing of glasses by filing an acrylic coating must be carried out before the surface state is too degraded.

References

[1] N. Bouaouadja, C. Bousbaa, T. Mahdaoui, H. Laouamri, and M.A. Madjoubi, Improvement of the optical transmission of an eroded soda lime glass by PVB and PES coatings, Physics Procedia, 2 (2009) 1351-1357.

[2] N. Pronk, B. Fildes, M. Regan, M. Lenné, N. Truedsson, and T. Olsson, Windscreens and safety A review, Monash University Accident Research Centre - Report #183, (2001).

[3] D.B. Mahadik, R.V. Lakshmi, and H.C. Barshilia, High performance single layer nano-porous antireflection coatings on glass by sol-gel process for solar energy applications, Solar Energy Materials and Solar Cells, 140 (2015) 61-68.

[4] D.C. Miller and S.R. Kurtz, Durability of Fresnel lenses: A review specific to the concentrating photovoltaic application, Solar Energy Materials and Solar Cells, 95 (2011) 2037-2068.

[5] K. Nishioka, K. Ikematsu, Y. Ota, and K. Araki, Sandblasting durability of acrylic and glass Fresnel lenses for concentrator photovoltaic modules, Solar Energy, 86 (2012) 3021-3025.

[6] N. Bouaouadja, M.A. Madjoubi, M. Kolli, C. Bousbaa, and M. Hamidouche, Etude des possibilités d'amélioration de la transmission optique d'un verre sodocalcique érodé par sablage, Verres Céramiques et Composites, 1 (2011) 43-51.

[7] M. Kolli, M. Hamidouche, N. Bouaouadja, and G. Fantozzi, HF etching effect on sandblasted soda-lime glass properties, Journal of the European Ceramic Society, 29 (2009) 2697-2704.

[8] M. Kolli, M.A. Madjoubi, M. Hamidouche, N. Bouaouadja, and G. Fantozzi, Amélioration de la résistance mécanique et de la transmission optique d'un verre sablé

par traitement chimique à l'acide fluorhydrique, Ann. Chim. Sci. Mat., 35 (2010) 129-136.

[9] H. Laouamri, M. Kolli, and N. Bouaouadja, Correction des défauts de sablage d'un verre par déposition de couches minces de silice et de PVB, Annales des Sciences et Technologie, 5 (2013) 136-142.

[10] C. Bousbaa, A. Madjoubi, M. Hamidouche, and N. Bouaouadja, Effect of annealing and chemical strengthening on soda lime glass erosion wear by sand blasting, Journal of the European Ceramic Society, 23 (2003) 331-343.

[11] I. Finnie, Erosion of surfaces by solid particles, Wear, 3 (1960) 87-103.

[12] I.M. Hutchings, Tribology : Friction and Wear of Engineering Materials, 1992.

[13] P.J. Slikkerveer, P.C.P. Bouten, F.H. in't Veld, and H. Scholten, Erosion and damage by sharp particles, Wear, 217 (1998) 237-250.

[14] R.H.M. Jafar, M. Papini, and J.K. Spelt, Simulation of erosive smoothing in the abrasive jet micro-machining of glass, Journal of Materials Processing Technology, 213 (2013) 2254-2261.

[15] M.A. Verspui, G. de With, A. Corbijn, and P.J. Slikkerveer, Simulation model for the erosion of brittle materials, Wear, 233–235 (1999) 436-443.

[16] N. Adjouadi, N. Laouar, C. Bousbaa, N. Bouaouadja, and G. Fantozzi, Study of light scattering on a soda lime glass eroded by sandblasting, Journal of the European Ceramic Society, 27 (2007) 3221-3229.

[17] S. Benterki, N. Laouar, C. Bousbaa, N. Bouras, and N. Bouaouadja, Influence of the angle of illumination on light scattering by sandblasted soda–lime–silica glass, Glass Technology - European Journal of Glass Science and Technology Part A, 53 (2012) 53-59.

[18] K.H. Holtmann, G.H. Frischat, and K. Ruppert, Mechanism of defect creation on sheet glass by particle impact and its influence on stray light, Glass Science and Technology, 71 (1988) 247-255.

[19] X. Gu, T. Nguyen, L.P. Sung, M.R. VanLandingham, M.J. Fasolka, J.W. Martin, Y.C. Jean, D. Nguyen, N.K. Chang, and T.Y. Wu, Advanced techniques for nanocharacterization of polymeric coating surfaces, JCT Research, 1 (2004) 191-200.

[20] M. Overend and C. Louter, The effectiveness of resin-based repairs on the inert strength recovery of glass, Construction and Building Materials, 85 (2015) 165-174.

[21] J.E. Ritter, Effect of Polymeric Coatings on Strength of Soda-Lime Glass, Fracture Mechanics of Ceramics, Springer, 1974, pp. 735-747.

[22] M. Wen, J.M. Chabagno, G. Silverman, and M. Bourrel, Edge-strengthening of flat glass with acrylate coatings, Journal of Non-Crystalline Solids, 354 (2008) 5060-5067.

[23] R. Prado, G. Beobide, A. Marcaide, J. Goikoetxea, and A. Aranzabe, Development of multifunctional sol–gel coatings: Anti-reflection coatings with enhanced self-cleaning capacity, Solar Energy Materials and Solar Cells, 94 (2010) 1081-1088.

[24] A. Baldan, Adhesion phenomena in bonded joints, International Journal of Adhesion and Adhesives, 38 (2012) 95-116.

[25] P. Richard, J. Thomas, D. Landolt, and G. Gremaud, Combination of scratch-test and acoustic microscopy imaging for the study of coating adhesion, Surface and Coatings Technology, 91 (1997) 83-90.

[26] W.G. Dorfeld, Bonding thermosprayed silicon to glass-ceramic, Thin Solid Films, 47 (1977) 241-247.

[27] C. Iliescu, J. Jing, F.E.H. Tay, J. Miao, and T. Sun, Characterization of masking layers for deep wet etching of glass in an improved HF/HCl solution, Surface and Coatings Technology, 198 (2005) 314-318.

[28] T.E. Myers, S. Shanmugam, T.S.I.I. Alan, M.J. Towner, K.W. Uhlig, and L. Zhang, Glass Etching Media And Methods, [Patent US20130299452 A1], 14-11-2013,

[29] L. Wong, T. Suratwala, M.D. Feit, P.E. Miller, and R. Steele, The effect of HF/NH4F etching on the morphology of surface fractures on fused silica, Journal of Non-Crystalline Solids, 355 (2009) 797-810.

[30] M. Barletta, S. Pezzola, S. Vesco, V. Tagliaferri, and F. Trovalusci, Experimental evaluation of plowing and scratch hardness of aqueous two-component polyurethane (2K-PUR) coatings on glass and polycarbonate, Progress in Organic Coatings, 77 (2014) 636-645.

[31] C. Gauthier and R. Schirrer, Time and temperature dependence of the scratch properties of poly(methylmethacrylate) surfaces, Journal of Materials Science, 35 (2000) 2121-2130.

[32] H. Jiang, R. Browning, and H.J. Sue, Understanding of scratch-induced damage mechanisms in polymers, Polymer, 50 (2009) 4056-4065.

[33] S.J. Bull and E.G. Berasetegui, An overview of the potential of quantitative coating adhesion measurement by scratch testing, Tribology International, 39 (2006) 99-114.

[34] V. Le Houérou, C. Gauthier, and R. Schirrer, Energy based model to assess interfacial adhesion using a scratch test, Journal of Materials Science, 43 (2008) 5747-5754.

[35] V. Jardret, H. Zahouani, J.L. Loubet, and T.G. Mathia, Understanding and quantification of elastic and plastic deformation during a scratch test, Wear, 218 (1998) 8-14.

[36] M. Kolli, H. Laouamri, M. Zaboub, and N. Bouaouadja, Improvement of the properties of sandblasted glass by acrylic coatings, Glass Technology: European Journal of Glass Science & Technology, 55 (2014) 146-152.

[37] M. Qiang, F. Chen, A. Zhou, S. Xiao, J. Zhang, and Z. Wang, Impacts of wind velocity on sand and dust deposition during dust storm as inferred from a series of observations in the northeastern Qinghai-Tibetan Plateau, China, Powder Technology, 175 (2007) 82-89.

[38] T. Mahdaoui, N. Bouaouadja, M. Madjoubi, and C. Bousbaa, Study of the Effects of Sand Blasting on Soda Lime Glass Erosion, International Review of Mechanical Engineering, 1 (2007) 502-510.

[39] P.V. Rao, Characterization of Optical and Surface Parameters During Particle Impact Damage, Journal of Engineering Materials and Technology, 108 (1986) 296-302.

[40] V. Jardret and P. Morel, Viscoelastic effects on the scratch resistance of polymers: relationship between mechanical properties and scratch properties at various temperatures, Progress in Organic Coatings, 48 (2003) 322-331.

[41] T.W. Seo and J.I. Weon, Influence of weathering and substrate roughness on the interfacial adhesion of acrylic coating based on an increasing load scratch test, Journal of Materials Science, 47 (2011) 2234-2240.

[42] M. Barletta, M. Puopolo, A. Gisario, and S. Vesco, Application and drying at ambient temperature of thick organic-inorganic hybrid coatings on glass, Surface and Coatings Technology, 236 (2013) 212-223.

[43] A. Baldan, Adhesively-bonded joints and repairs in metallic alloys, polymers and composite materials: Adhesives, adhesion theories and surface pretreatment, Journal of Materials Science, 39 (2004) 1-49.

Oxides	SiO_2	Na_2O	CaO	MgO	Al_2O_3	Fe_2O_3	K_2O	SO_3	others
Mass %	69.14	13.20	8.33	3.97	1.77	0.2	0.83	0.69	1.97

Table 1: *Mean chemical composition of the glass.*

Mass of projected sand	**Projected mass density**	**Kinematic energy density**
g	*g/cm²*	*mJ/mm²*
50	4	12.5
100	8	25
150	12	37.5
200	16	50

Table 2: *Sandblasting levels of the specimens.*

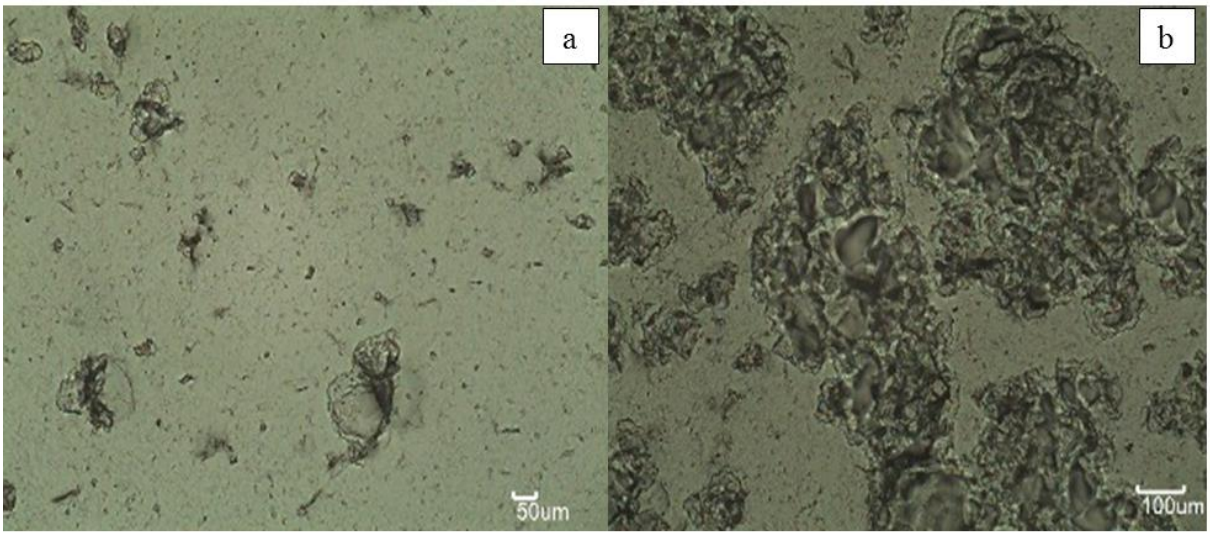

Figure 1: *Micrographs of sandblasted glasses with: (a) Mp=50 g, (b) Mp=200g.*

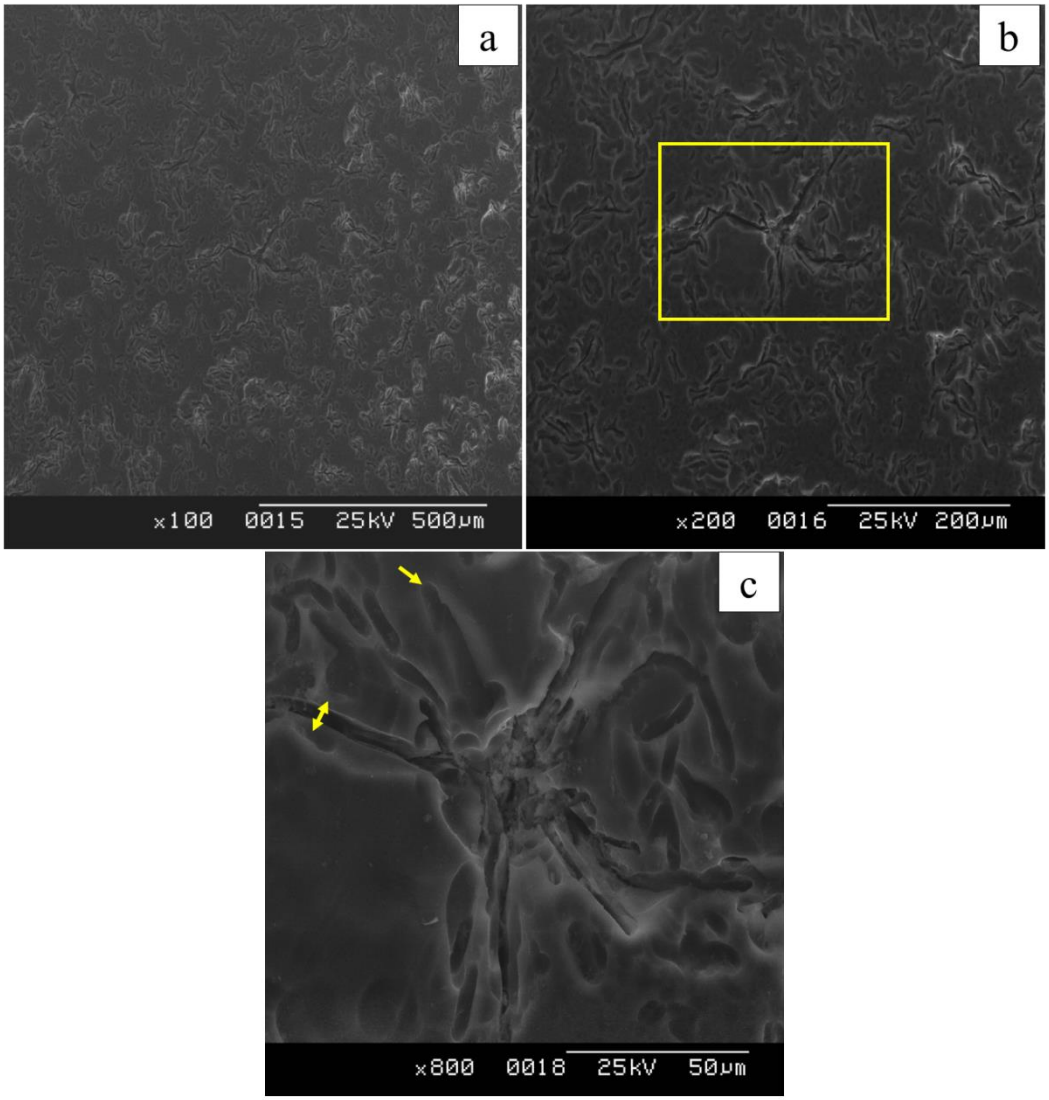

Figure 2: *SEM micrographs showing erosion defects on sandblasted surface submitted to chemical attack during 2 min with different magnifications: a) x100, b) x200 and c) x800. Arrows in c) indicate examples of cracks blunting.*

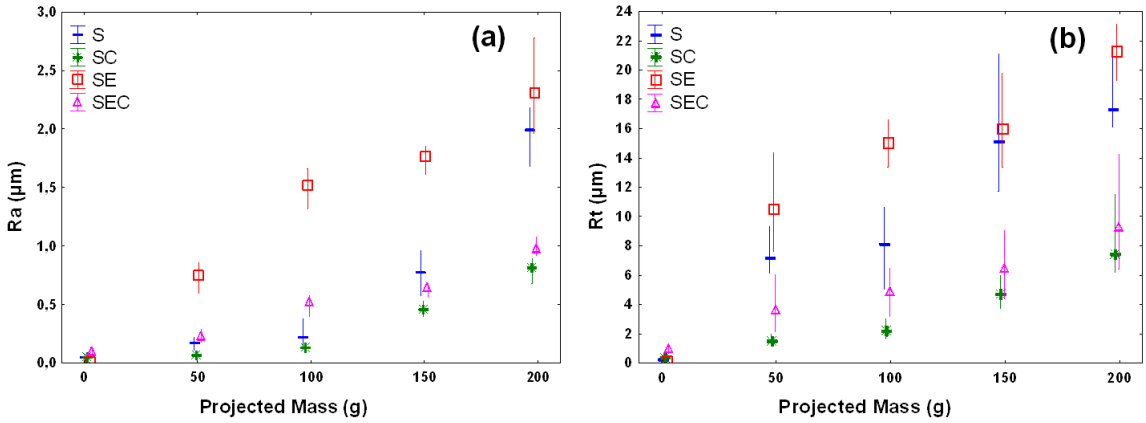

Figure 3: *Variation of surface roughness parameters Ra (a) and Rt (b) before and after depositing acrylic coatings with or without etching (S = sandblasted glass; C = coated; E = etched).*

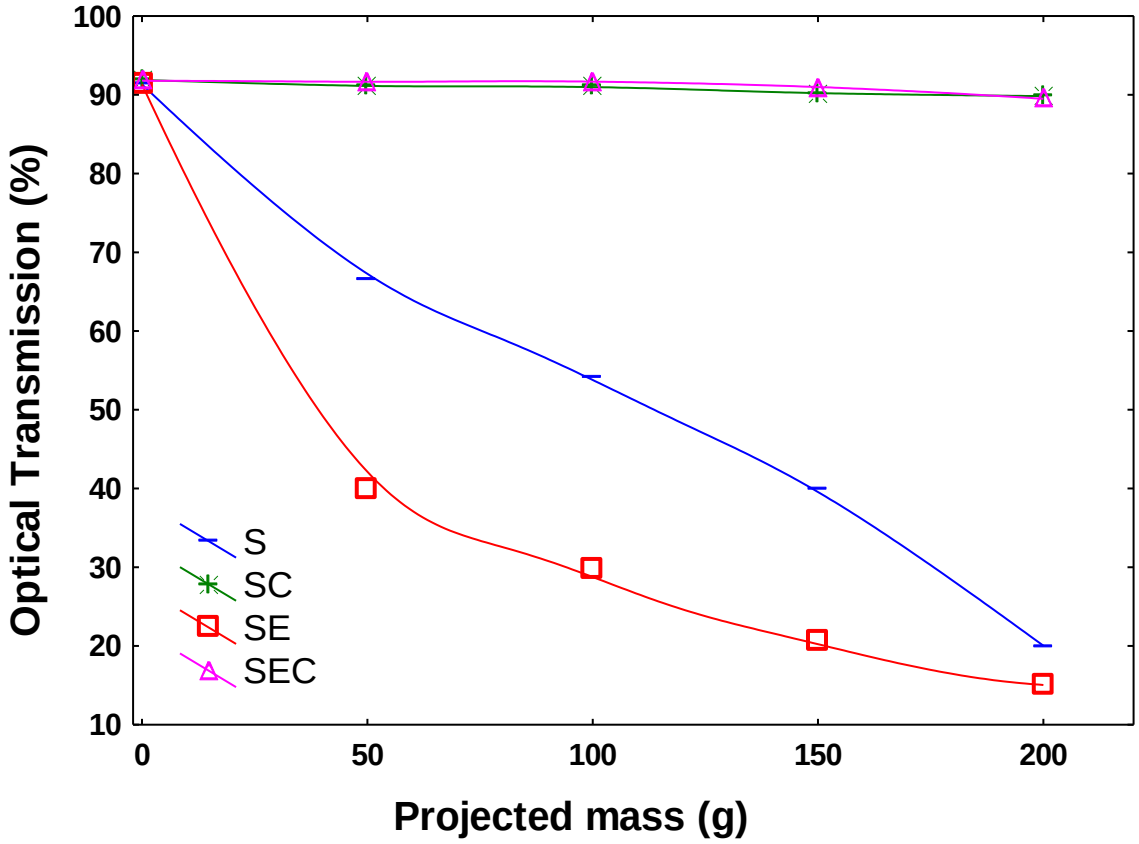

Figure 4: *Variation of the optical transmission (λ = 550 nm) as a function of the projected sand mass for different glass states (S = sandblasted glass; C = coated; E = etched).*

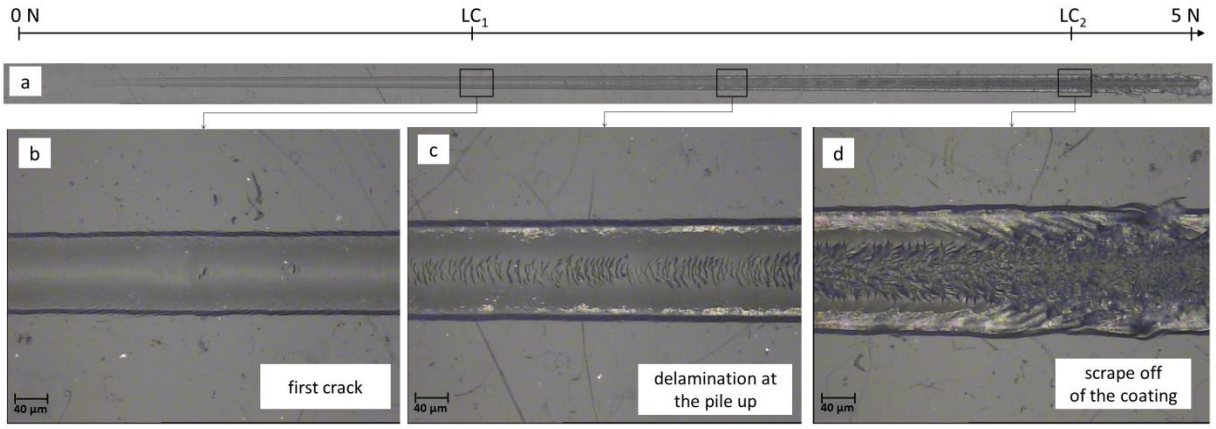

Figure 5: *(a) Scratch example of specimen 050SC (sandblasted specimen with 50g of sand and coated): (b) definition of LC_1, (c) delamination at the pile up and (d) definition of LC_2.*

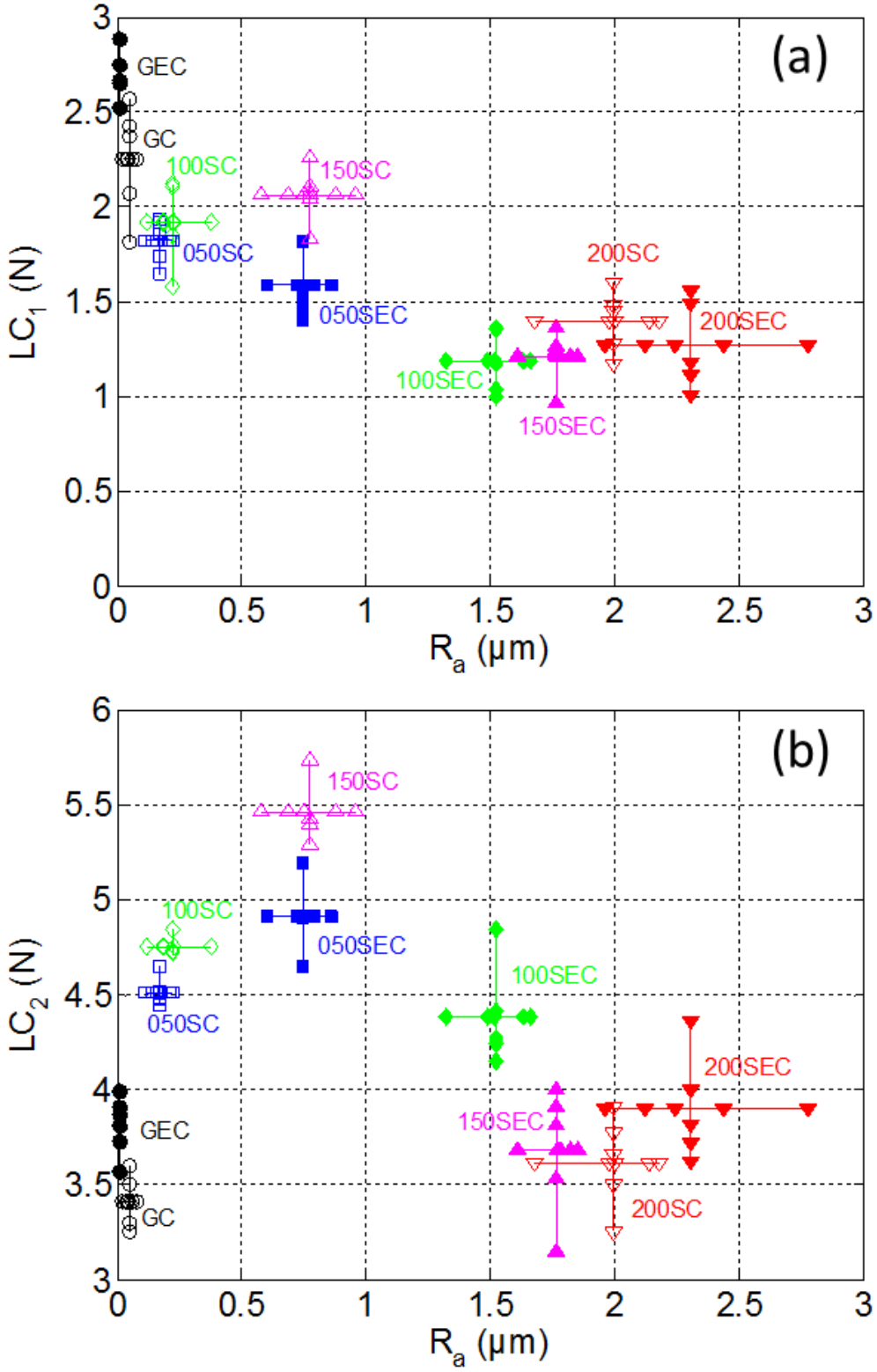

Figure 6: *Critical loads LC_1 (a) and LC_2 (b) vs. arithmetic roughness measured on uncoated specimens (G = as received glass; E = etching; C = coating; S = sandblasted glass; number = mass of sand in grams).*